Temperature dependence of the optical phonons and transverse effective charge in 3C-SiC

Diego Olego and Manuel Cardona

Max-Planck-Institut für Festkörperforschung, Heisenbergstrasse 1, 7000 Stuttgart 80, Federal Republic of Germany

(Received 28 August 1981)

The temperature dependence of the long-wavelength optical phonons of 3C-type SiC has been measured for temperatures up to 750 K. The LO-TO splitting diminishes with increasing temperature. From these data a weak decrease of the transverse effective charge with increasing temperature is also derived. The "explicit" temperature contribution to the variation of the transverse effective charge is determined experimentally and calculated in terms of a pseudopotential expression for the charge. Good agreement between theory and experiment is achieved.

I. INTRODUCTION

The influence of anharmonic interactions on the lattice vibrations can be experimentally studied by measuring changes of phonon self-energies with temperature. Renormalization of phonon frequencies and phonon lifetimes with increasing temperature are measurable with spectroscopic techniques such as Raman scattering or infrared absorption. Though neutron scattering allows the whole-phonon dispersion curves to be determined, its accuracy is in most of the cases not enough to measure differential effects.

The temperature dependence of the first-order Raman lines has been studied in detail for materials with diamond structure: Si,[1]Ge,[2,3] and diamond.[4,5] Some data also exist for SiC, ZnO, and ZnS in the wurtzite structure.[6] In all cases, softening of the optical frequencies at the zone center and broadening of the one-phonon Raman lines were observed as the temperature was increased. For Si and Ge the measured temperature shifts of the long-wavelength optical phonons to lower energies are described quantitatively by Cowley's theoretical calculations.[1,2,3,7] The increase of the linewidth of the one-phonon Raman line has been attributed to the decay of the zone-center optical phonon into two longitudinal acoustical ones.[1] The energy of these LA phonons is one-half of that of the optical phonon and their wave vectors are of equal magnitude but opposite signs in order to ensure momentum conservation. The decay process results from the coupling between the phonon normal modes introduced by third-order anharmonic interactions.

The purpose of this paper is to present the results of the temperature dependence of the long-wavelength optical phonons of zinc-blende 3C-type SiC measured with first-order Raman scattering. Particular emphasis is given to the dependence of the transverse effective charge e_T^* on temperature. We report a decrease of the LO(Γ)-TO(Γ) splitting when the temperature is increased from 80 to 730 K. However, the corresponding transverse effective charge remains almost constant because of the positive temperature coefficient of the high-frequency dielectric constant ϵ_∞. The increase of ϵ_∞ with increasing temperature counteracts the decrease of the LO(Γ)-TO(Γ) splitting.

The measured coefficient $(\partial e_T^*/\partial T)_p$ (derivative of e_T^* with respect to the temperature T at constant pressure p) together with the behavior of e_T^* upon lattice compression reported in the preceding paper allow us to determine the so-called "explicit" contribution $(\partial e_T^*/\partial T)_V$ (derivative of e_T^* with respect to T at constant volume V).

We discuss this explicit contribution in terms of the simplified pseudopotential expression for e_T^*,[8] which has been tested in the preceding paper and found to be suitable to describe differential effects on the effective transverse charge of 3C-SiC. The intrinsic temperature dependence of e_T^* is calculated by assuming that the perturbation in the pseudopotential form factors produced by the temperature is given by Debye-Waller factors.[9] This procedure has been successfully applied to describe temperature effects on the electronic band edges[9] and on optical properties such as the refractive index.[10] The calculated value of the intrinsic temperature coefficient of e_T^* agrees in order of magnitude and sign with the experiment.

II. EXPERIMENTAL DETAILS

The Raman measurements were performed in backscattering by using the same samples, laser line, monochromator, and detection system described in Sec. II of the preceding paper. For the low-temperature measurement (77 K) the 3C-SiC sample was mechanically mounted on a copper cold finger which was placed in an evacuated glass Dewar in contact with liquid nitrogen. The high-temperature measurements ($T > 300$ K) were performed with the sample held in mechanical contact with a heated copper block also placed in an evacuated glass Dewar. The temperature was measured with a NiCr-Ni thermocouple brought near the sample. The accuracy in the determination of the temperature was ± 1 K.

III. RESULTS AND DISCUSSION

Typical first-order Raman spectra of 3C-SiC recorded for two different temperatures are shown in Fig. 1. With increasing temperature the LO and TO Raman lines shift to lower frequencies and become broadened. The wave number scales of Fig. 1 have been drawn to display the fact that the shifts of the LO line to lower frequencies are larger than those of the TO line and, consequently, that a decrease of the LO(Γ)-TO(Γ) splitting with

increasing temperature takes place.

The measured peak positions of the LO and TO lines as a function of temperature are plotted in Fig. 2. For temperatures larger than 300 K a linear dependence is observed. Departures of linearity at low temperatures have also been measured in Si,[1] Ge,[2,3] and α-SiC.[6] The solid lines drawn in Fig. 2 through the experimental points are linear least-squares fits to the data for $T > 300$ K. The temperature coefficients at constant pressure obtained from these fits are tabulated in Table I and compared with those reported for α-SiC. Cowley has performed a numerical calculation of the frequency shifts of the long-wavelength optical phonons of diamond, Si, and Ge.[7] We compared in Fig. 3 the value of $\frac{1}{2}(\omega_{Si} + \omega_C)$ from his results with the weighted value $\frac{1}{3}(2\omega_{TO} + \omega_{LO})$ obtained from the data of Fig. 2. The calculated mean value between Si and C has been normalized to the measured weighted value of 3C-SiC at $\simeq 300$ K. As was the case for Ge and Si, the calculated shifts agree well with the experimental ones.

The data plotted in Fig. 2 show that the LO(Γ)-TO(Γ) splitting decreases with increasing temperature. The behavior of this splitting as the temperature increases is displayed in Fig. 4. Although the decrease of the LO(Γ)-TO(Γ) splitting with temperature is small as compared with the changes produced by hydrostatic pressure (see preceding paper), it is well beyond the experimental uncertainty.
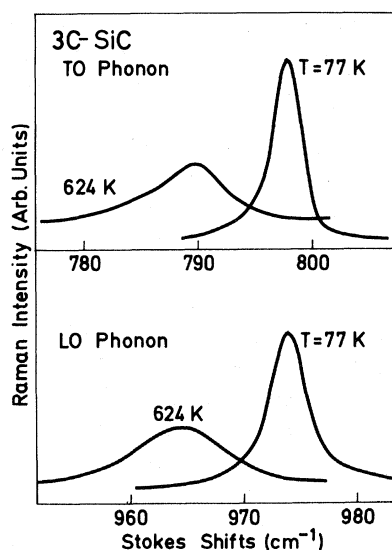

FIG. 1. First-order Raman lines recorded at two different temperatures. With increasing temperature the lines shift to lower frequencies and broaden. The shifts of the LO line are stronger than those of the TO line.
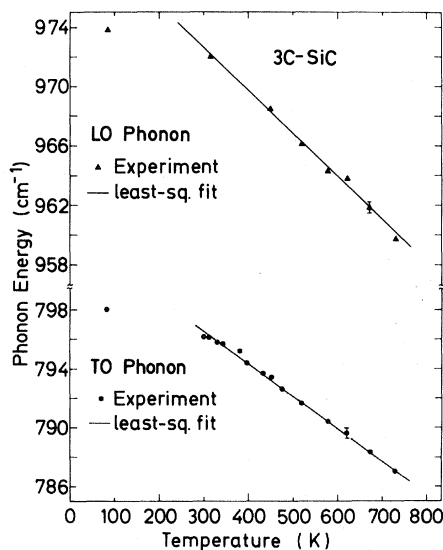

FIG. 2. Temperature dependence of the peak positions of the LO and TO Raman lines. The solid lines are linear least-squares fits to the experimental data for temperatures larger than 300 K.

TABLE I. Temperature coefficients of the long-wavelength optical phonons of α- and 3C-types SiC.

Type	$\left[\dfrac{d\omega_{TO}}{dT}\right]_p$ $(10^{-2}\ cm^{-1}K^{-1})$	$\left[\dfrac{d\omega_{LO}}{dT}\right]_p$ $(10^{-2}\ cm^{-1}K^{-1})$	$\left[\dfrac{d(\omega_{LO}-\omega_{TO})}{dT}\right]_p$ $(10^{-2}\ cm^{-1}K^{-1})$
3C-SiC[a]	$-(2.18\pm0.03)$	$-(2.90\pm0.03)$	$-(0.71\pm0.06)$
α-SiC[b]	$-(3.0\ \pm0.2)$	$-(3.1\ \pm0.2)$	$\simeq 0$

[a]This work.

[b]Reference 6. In the case of α-SiC, ω_{TO} refers to the $E_1(TO)$ mode and ω_{LO} to the $A_1(LO)$ mode.

Again we performed a linear least-squares fit to the experimental points for T larger than 300 K. The solid line of Fig. 4 represents the results of this fit. The temperature coefficient of the LO(Γ)-TO(Γ) splitting is given in Table I. It is interesting to note that we measure a change of the splitting in 3C-SiC while the $A_1(LO)$-$E_1(TO)$ splitting in α-SiC is independent of temperature.[6] As is the case of 3C-SiC, the splitting is due to electrostatic forces which dominate over the anisotropy of the short-range forces.[11]

The temperature dependence of the linewidths of the one-phonon Raman spectra is presented in Fig. 5. The data have been corrected for the instrumental resolution by assuming Gaussian slit functions and line shapes with the procedure described

in Ref. 3. The increase of the linewidths with increasing temperature in the cases of Si (Ref. 1) and Ge (Refs. 2 and 3) could be explained by assuming that the lifetime of the optical phonon is determined by a decay process into two LA phonons of half their energy. Hence the temperature dependence of the linewidth W is given by

$$W(T)=W(0)[1+2/(e^x-1)]\ , \qquad (1)$$

with $W(0)$ the linewidth at $T=0$. In Eq. (1) $x=\hbar\omega/kT$ where $\hbar\omega$ represents the energy of the optical mode under consideration. The solid lines in Fig. 5 represent the best fits to the experimental results performed with Eq. (1) using $W(0)$ as a fitting parameter. For the TO-phonon Raman line we obtained $W(0)=2\pm0.2\ cm^{-1}$ with $\hbar\omega=796$ cm^{-1}. In the case of the LO-phonon Raman line, with $\hbar\omega=972\ cm^{-1}$, we found $W(0)=3.8\pm0.2$ cm^{-1}. The agreement between the experiment and the fits with Eq. (1) is good for temperatures up to 600 K. For the highest temperatures the experimental points lie somewhat above the calculated
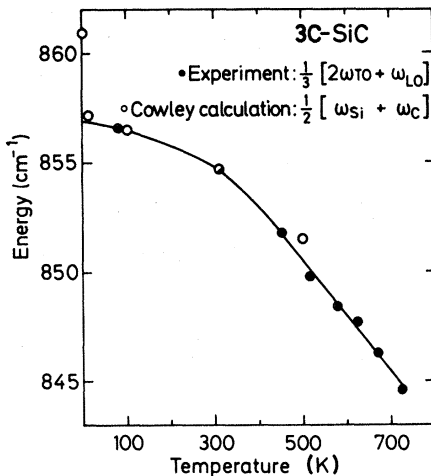

FIG. 3. Comparison between the mean values of the calculated shifts of ω_{LO} and ω_{TO} for Si and diamond (Ref. 7) and the corresponding measured values for 3C-SiC. The calculated weighted mean value for $T\simeq300$ K has been normalized to the experimental one. The solid line through the experimental data (heavy dots) has been drawn as a visual aid.

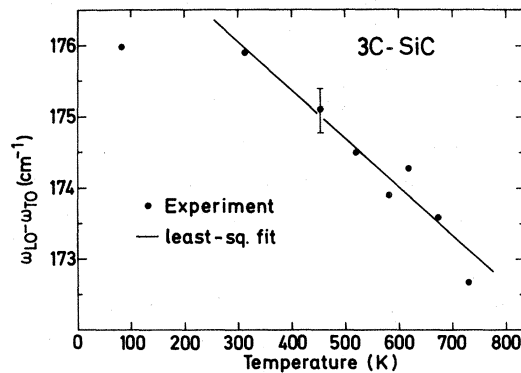FIG. 4. Temperature dependence of the LO(Γ)-TO(Γ) splitting. The solid line represents a linear least-squares fit to the experimental points for T larger than 300 K.
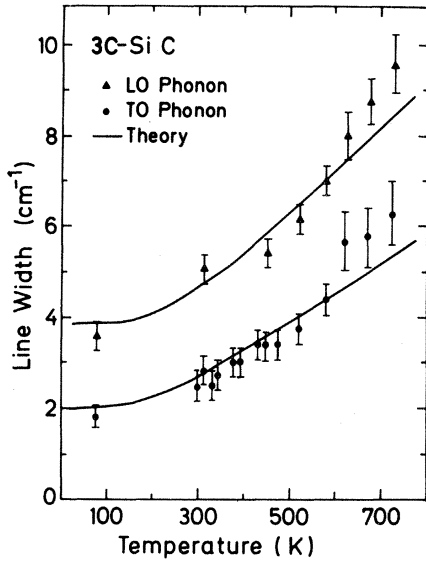
FIG. 5. Temperature dependence of the linewidths of the TO- and LO-phonon Raman lines. The measured linewidths have been corrected for instrumental resolution. The solid lines are the best fits obtained with Eq. (1).

curves. This discrepancy may arise from the procedure used to correct for instrumental resolution. Under the assumption of Lorentzian line shapes the corrected linewidths at very high temperatures become smaller.

IV. TRANSVERSE EFFECTIVE CHARGE e_T^*

In Sec. IV of the preceding paper we have discussed the relationship between the LO(Γ)-TO(Γ) splitting and the Born's transverse effective charge e_T^*. This relationship is given by

$$e_T^{*2} = \frac{a^3 \epsilon_\infty M_{red}}{16\pi} [\omega_{LO}^2(\Gamma) - \omega_{TO}^2(\Gamma)] , \qquad (2)$$

where a is the lattice constant, ϵ_∞ the high-frequency dielectric constant, and M_{red} the reduced mass of the Si and C atoms. e_T^* depends on temperature not only through ω_{LO}, ω_{TO}, and a thermal dilatation but also through the temperature dependence of ϵ_∞. In the case of 3C-SiC this dependence has not been measured. However, data exist for Si and diamond, from which a mean value $(1/\epsilon_\infty)(\partial \epsilon_\infty/\partial T)_p \simeq 5 \times 10^{-5}$ K^{-1} results.[9,10] This value is a factor of 2 larger than the temperature coefficient one can calculate from the existing data for α-SiC by averaging ϵ_∞ parallel and perpendicu-

lar to the c axis.[12] The measurements reported in Ref. 12 have been performed at $T = 105$ K and $T = 297$ K. Within this temperature range the dependence of the band edges on temperature is weaker than at higher temperatures when it becomes linear.[13] As the temperature dependence of the dielectric constant is mostly due to the dependence of the so-called Penn gap (see below),[9,10] we believe that the value of 5×10^{-5} K^{-1} for $(1/\epsilon_\infty)$ $\times (\partial \epsilon_\infty/\partial T)_p$ is appropriate for the temperature range of interest. The lattice constant can be expressed as follows:

$$a = a_0(1 + \Delta a/a_0) , \qquad (3)$$

with $a_0 = a(T = 300$ K$)$, and $\Delta a/a_0$ the linear thermal expansion, which is tabulated as a function of temperature for SiC in Ref. 14.

Figure 6 displays the temperature dependence of e_T^* obtained with Eq. (2) by using the measured LO and TO frequencies at different temperatures, the linear latter expansion as given in Ref. 14, and the discussed temperature coefficient of ϵ_∞. To evaluate Eq. (2) we used for $T \simeq 300$ K, $a_0 = 4.3596$ Å and $\epsilon_\infty = 6.52$.[15] We have taken into consideration only the temperatures larger than 300 K to avoid the nonlinearity in the temperature dependence of the LO and TO phonons (Fig. 2) and possible nonlinearities in the dependence of ϵ_∞ on temperature. Although the experimental scatter is very large, a weak decrease of e_T^* with increasing temperature can be ascribed to the data of Fig. 6 (the reader should note how much expanded the vertical scale is in comparison with that of Fig. 5 of the preceding paper). The solid line drawn through the points represents the linear least-squares fit,

$$e_T^* = 2.692 \pm 0.002$$

$$-(9 \pm 0.5) \times 10^{-6}(T - 300 \text{ K}) . \qquad (4)$$

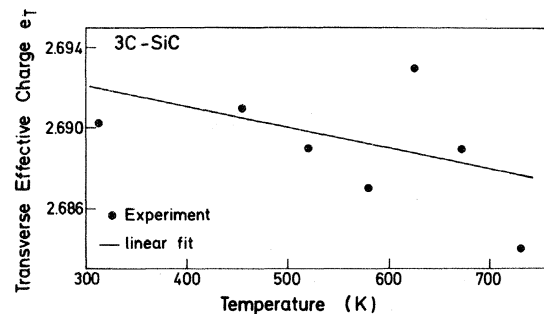The value of e_T^* for $T = 300$ K agrees within the

FIG. 6. Temperature dependence of the transverse effective charge. The solid line is a linear fit with Eq. (4).

experimental error with $e_T^* = 2.697 \pm 0.004$ reported for zero lattice compression in the preceding paper. The temperature dependence of e_T^*, as given by Eq. (4), is weaker than that of $(\omega_{LO}^2 - \omega_{TO}^2)^{1/2}$ with the coefficients tabulated in Table I. This is because of the opposite temperature dependences of the LO-TO splitting and the high-frequency dielectric constant. From Eq. (4) we obtain a value for the derivative of e_T^* with respect to the temperature at constant pressure

$$\left[\frac{\partial e_T^*}{\partial T} \right]_p = -(9 \pm 0.5) \times 10^{-6} \text{ K}^{-1} . \qquad (5)$$

This coefficient includes the contributions of two terms:

$$\left[\frac{\partial e_T^*}{\partial T} \right]_p = \left[\frac{\partial e_T^*}{\partial T} \right]_V + \alpha \left[\frac{\partial e_T^*}{\partial \frac{\Delta a}{a_0}} \right]_T , \qquad (6)$$

with α the linear expansion coefficient. The first term on the right-hand side (derivative of e_T^* with respect to T at constant volume V) described the so-called "explicit" temperature contribution to the dependence of e_T^* on T; the second accounts for the thermal expansion. Because of the relationship between e_T^* and the electronic band structure of the material [see Eq. (11) in the preceding paper] the "explicit" contribution is directly related to the electron-phonon interaction, which also plays a very important role in the temperature dependence of the band edges.[16] With

$$\left[\frac{\partial e_T^*}{\partial \frac{\Delta a}{a_0}} \right]_T = -(5.45 \pm 0.10)$$

(preceding paper) and $\alpha \simeq (4 \pm 1) \times 10^{-6} \text{ K}^{-1}$ [Ref. 14 and Eq. (5)], we obtain from Eq. (6)

$$\left[\frac{\partial e^*}{\partial T} \right]_V = (1.28 \pm 0.5) \times 10^{-5} \text{ K}^{-1} . \qquad (7)$$

We present now a calculation of this "explicit" temperature contribution in terms of the pseudopotential model for the transverse efffective charge.[8,17] The complete pseudopotential expression for e_T^* [Eq. (4.6) of Ref. 17 and Eq. (11) of the preceding paper] can be simplified if one keeps the psudopotential form factors only up to $G = (2\pi/a)\sqrt{8}$ and applies a Heine and Jones[18] band-structure model [see Eqs. (A7) and (A8) in Ref. 8]

$$e_T^* = -\Delta Z - \frac{8}{E_g} \left\{ \frac{1}{2}[v_{Si}(8) - v_C(8)] + \frac{1}{2E_x}[v_{Si}^2(3) - v_C^2(3)] \right\} ,$$

with $\qquad (8)$

$$E_g = v_{Si}(8) + v_C(8) + \frac{1}{E_x}[v_{Si}^2(3) + v_C^2(3)] , \qquad (9)$$

and

$$E_x = \frac{1}{2}(2\pi/a)^2 . \qquad (10)$$

The v's are the pseudopotential atomic form factors taken at the reciprocal-lattice vectors $G = (2\pi/a)\sqrt{3}$ and $(2\pi/a)\sqrt{8}$ (see Fig. 5 in preceding paper). We note that Eq. (8) goes over into Eq. (16) of the preceding paper if we neglect the $v(8)$'s. In the present work we found it necessary to retain these terms in order to account for the observed temperature dependence of e_T^* (see below). We recall that for SiC $\Delta Z = 0$.

With Eqs. (8) and (9) we calculate the temperature dependence of e_T^* by assuming that the perturbation produced by the temperature can be taken into account by multiplying the Fourier component of the pseudopotential v's by the appropriate Debye-Waller factor[9,10]:

$$v(G,T) = v(G)e^{-G^2\langle u^2 \rangle/6} \simeq v(G)(1 - \frac{1}{6}G^2\langle u^2 \rangle) , \qquad (11)$$

with $\langle u^2 \rangle$ the mean-square displacement of the corresponding atom. This method has been successfully used to calculate the temperature coefficients of band edges and long-wavelength refractive index.[9,10] Equation (11) gives the average potential in the presence of thermal agitation which has the translational invariance of the static lattice. It corresponds to taking into account the second-order electron-phonon interaction as first-order perturbation theory. Strictly speaking, one should also include first-order electron-phonon terms in second-order perturbation theory. There is, however, a considerable amount of evidence that the latter terms are negligible in the pseudopotential representation, at least for calculating the temperature dependence of energy gaps and polarizabilities of tetrahedral semiconductors.[9,10,16] In view of the difficulties involved in including them we shall also neglect them here. The correctness of this procedure is confirmed by the agreement found with the experimental results.

TABLE II. Atomic pseudopotential form factors (in Ry) and their temperature deriva-
tives used to evaluate the transverse effective charge and its temperature dependence.

G	v_{Si}	v_C	$\dfrac{\partial v_{Si}}{\partial T}$ (10^{-6} K^{-1})	$\dfrac{\partial v_C}{\partial T}$ (10^{-6} K^{-1})
$3^{(a)}$	-0.218	-0.460	3.85	7.17
$8^{(a)}$	0.172	-0.126	-8.10	5.24
$3^{(b)}$	-0.190	-0.55	3.35	8.56
$8^{(b)}$	0.150	-0.03	-7.06	1.25

[a]Fitted to SiC; see preceding paper.
[b]From M. L. Cohen and T. K. Bergstresser, Ref. 21, renormalized as discussed in the
preceding paper.

We use the expression for e_T^* given by Eq. (8) in-
stead of the "first-order approximation" given by
Eq. (16) of the preceding paper for two reasons:
First, Eq. (8) includes explicitly an effective gap
E_g. We shall see later that the temperature depen-
dence of this gap determines that of e_T^*. It reflects
in part the influence of the dielectric constant in
Eq. (2). Second, we can see from Eq. (11) that the
Debye-Waller factor is more important the larger
the value of G. Consequently, the contributions of
the pseudopotential form factors $v(8)$ and their
derivatives with respect to T should be included.

From Eq. (11) we have

$$\left[\frac{\partial v(G,T)}{\partial T} \right]_V = -\frac{1}{6} v(G) G^2 \frac{\partial \langle u^2 \rangle}{\partial T} . \qquad (12)$$

To our knowledge no measurements of $\langle u^2 \rangle$ as a
function of temperature are available for 3C-SiC.
However, theoretical calculations have been per-
formed for a number of zinc-blende-type materials
including 3C-SiC.[19] In the case of 3C-SiC the cal-
culation predicts a linear dependence of $\langle u^2 \rangle$ with
temperature for T larger than 250 K, with the fol-
lowing coefficients for the Si and C atoms:

$$\frac{\partial \langle u_{Si}^2 \rangle}{\partial T} = 6.07 \times 10^{-5} (R_B)^2 \text{ K}^{-1} ,$$

$$\frac{\partial \langle u_C^2 \rangle}{\partial T} = 5.36 \times 10^{-5} (R_B)^2 \text{ K}^{-1} , \qquad (13)$$

where R_B stands for the Bohr radius. The values

of the atomic pseudopotential form factors and the
derivatives with respect to T evaluated with Eqs.
(12) and (13) are presented in Table II (see also
preceding paper).

Before we calculate the temperature dependence
of E_T^* we evaluate E_g for 3C-SiC and its derivative
with respect to T in order to test the validity of the
approximation. With $a = 4.3596$ Å $= 8.24$ a.u. and
the pseudopotential (a) in Table II we obtain with
Eq. (9): $E_g = 0.937$ Ry$= 12.7$ eV. This effective
gap can be identified with the Penn gap[18] (approxi-
mately the gap at the X point of the Brillouin
zone). For energies near E_g the strongest peak
takes place in the oscillator strength and the reflec-
tivity of the group-IV and group-III-V semicon-
ductors.[9] An "experimental" value for E_g can be
obtained from the relation[9]

$$\epsilon(0) \simeq 1 + \left[\frac{\hbar \omega_p}{E_g} \right]^2 , \qquad (14)$$

with $\epsilon(0)$ the static dielectric constant and ω_p the
plasma frequency of the valence electrons (~ 16
eV). With $\epsilon(0) = 9.72$ (Ref. 15), $E_g \simeq 8$ eV. The
agreement between the value calculated with Eq.
(9) for the (a) pseudopotentials of Table II and the
"experimental" one of relation (14) is satisfactory.
For Si and C similar calculations for E_g give
values which are larger than those obtained with
Eq. (14).[10] The result obtained for 3C-SiC if the (b)
pseudopotentials are used is $E_g = 1.28$ Ry$\simeq 17$ eV.

The temperature dependence of E_g is, from Eq.
(9) and the data of Table II:

$$\left[\frac{\partial E_g}{\partial T} \right]_V = \frac{\partial v_{Si}(8)}{\partial T} + \frac{\partial v_C(8)}{\partial T} + \frac{2}{E_x} \left[v_{Si}(3) \frac{\partial v_{Si}(3)}{\partial T} + v_C(3) \frac{\partial v_C(3)}{\partial T} \right]$$

$$= -3.13 \times 10^{-5} \text{ Ry K}^{-1} = -4.3 \times 10^{-4} \text{ eV K}^{-1} \text{ for (a) pseudopotentials} .$$

$$= -3.4 \times 10^{-5} \text{ Ry K}^{-1} = -4.6 \times 10^{-4} \text{ eV} K^{-1} \text{ for (b) pseudopotentials} .$$

The order of magnitude and the sign of $(\partial E_g/\partial T)_V$ are in both cases in good agreement with the temperature coefficients measured and calculated for other zinc-blende-type semiconductors.[9,10]

We evaluate now the transverse effective charge. With Eq. (8) the results are $e_T^* = 1.14$ for case (a) in Table II and $e_T^* = 2.31$ for case (b). The calculated value for the charge in case (a) is approximately a factor of 2 smaller than the experimental one [Eq. (4)]. For case (b) the agreement is much better. It is known that the transverse effective charges do not show a strong chemical trend (one finds $e_T^* \simeq 2$ for almost all semiconductors).[20] However, the differential effects depend on the material and a good test of a model is how it describes such differential effects.

To characterize the contributions to the temperature dependence of e_T^*, we write Eq. (8) in the following form:

$$e_T^* = -\frac{1}{E_g}A \ , \tag{15}$$

with

$$A = 8\left[\frac{1}{2}[v_{Si}(8)-v_C(8)]+\frac{1}{2E_x}[v_{Si}(3)-v_C(3)]\right] = -1.068 \ \text{Ry} \quad \text{for (a) pseudopotentials}$$

$$= -2.95 \ \text{Ry} \quad \text{for (b) pseudopotentials}$$

and

$$\left[\frac{\partial A}{\partial T}\right]_V = 8\left[\frac{1}{2}\left[\frac{\partial v_{Si}(8)}{\partial T}-\frac{\partial v_C(8)}{\partial T}\right]+\frac{1}{E_x}\left[v_{Si}(3)\frac{\partial v_{Si}(3)}{\partial T}-v_C(3)\frac{\partial v_C(3)}{\partial T}\right]\right]$$

$$= 1.42\times10^{-5} \ \text{Ry}\,\text{K}^{-1} \quad \text{for (a) pseudopotentials}$$

$$= 7.8\times10^{-5} \ \text{Ry}\,\text{K}^{-1} \quad \text{for (b) pseudopotentials} \ ,$$

using the values of Table II. Hence

$$\left[\frac{\partial e_T^*}{\partial T}\right]_V = e_T^*\left[\frac{-1}{E_g}\frac{\partial E_g}{\partial T}+\frac{1}{A}\frac{\partial A}{\partial T}\right]$$

$$= (3.8-1.5)\times10^{-5} \ \text{K}^{-1} = 2.3\times10^{-5} \ \text{K}^{-1} \quad \text{for (a) pseudopotentials} \ ,$$

$$= (6.15-6.10)\times10^{-5} \ \text{K}^{-1} = +0.05\times10^{-5} \ \text{K}^{-1} \quad \text{for (b) pseudopotentials} \ .$$

The first term in large parentheses comes from the temperature dependence of the effective gap and determines the sign of the intrinsic contribution to the dependence of e_T^* on temperature. The agreement between the experimental value (1.28 ± 0.5) $\times10^{-5}$ and the calculated one is good in case (a) if one considers that pressure effects are described by the model with the same accuracy. In particular, we have been able to interpret theoretically the observed sign of $(\partial e^*/\partial T)_V$. For the pseudopotential set (b) the same sign is obtained; the magnitude of the calculated effect, however, is too small. The main reason for that is the anomalously large value

of E_g (17 eV) obtained with this set of pseudopotentials.

V. CONCLUSIONS

We have shown that the temperature dependence of the long-wavelength optical phonons of 2C-SiC can be understood along lines similar to those followed for other group-IV semiconductors. The model that attributes the lifetimes of the optical phonons to a decay into two LA phonons seems to apply also for 3C-SiC. We reported the observa-

tion of a decrease of the LO-TO splitting with increasing temperature and also a corresponding decrease of the transverse effective charge. However, the dependence of e_T^* on temperature is weaker than that of the LO-TO splitting because of a cancellation with the temperature dependence of the high-frequency dielectric constant. By combining the temperature and pressure data the "explicit" temperature contribution to the dependence of e_T^* on temperature was determined. We were able to calculate this contribution by applying Debye-Waller coefficients to the pseudopotential expression for e_T^*. In doing so, we have used for the case of the effective charge, the ideas developed to calculate temperature effects on band edges and related properties. It was shown that the main contribution to the intrinsic temperature coefficient of e_T^* comes from the effective Penn gap. The capability of the pseudopotential method to describe differential effects had been also confirmed.

ACKNOWLEDGMENTS

[1] T. R. Hart, R. L. Aggarwal, and B. Lax, Phys. Rev. B 1, 638 (1970).

[2] R. K. Ray, R. L. Aggarwal, and B. Lax, in Light Scattering in Solids, edited by M. Balkanski (Flammarion Sciences, Paris, 1971) p. 288.

[3] F. Cerdeira and M. Cardona, Phys. Rev. B 5, 1440 (1972).

[4] S. A. Solin and A. K. Ramdas, Phys. Rev. B 1, 1687 (1970).

[5] R. S. Krishnan, Proc. Indian Acad. Sci. 24, 45 (1946).

[6] D. G. Mead and G. R. Wilkinson, J. Raman Spectros. 6, 123 (1977).

[7] R. A. Cowley, J. Phys. (Paris) 26, 659 (1965).

[8] R. Trommer, H. Müller, M. Cardona, and P. Vogl, Phys. Rev. B 21, 4869 (1980).

[9] M. Cardona, in Atomic Structure and Properties of Solids, edited by E. Burstein (Academic, New York, 1972) p. 514.

[10] P. Y. Yu and M. Cardona, Phys. Rev. B 2, 3193 (1970).

[11] G. R. Wilkinson, in The Raman Effect, edited by A. Anderson (Dekker, New York, 1973), Vol. 2, p. 811.

[12] A. N. Pikhtin, V. N. Prokopenko, V. S. Rondarev, and A. D. Yaskov, Opt. Spectrosk. 43, 711 (1977).

[13] D. Olego and M. Cardona, Phys. Rev. B 22, 886 (1980).

[14] Thermophysical Properties of Matter, Vol. 13 of The TPRC Data Series, edited by Y. Touloukian, R. Kirby, R. Taylor, and T. Lee (Plenum, New York, 1977).

[15] See, for example, Appendix II of Silicon Carbide 1973, edited by R. C. Marshall, J. W. Faust, and C. E. Ryan (University of South Carolina Press, City 1974), and references therein.

[16] P. B. Allen and M. Cardona, Phys. Rev. B 23, 1495 (1981); 24, 7479 (E) (1981).

[17] P. Vogl, J. Phys. C 11, 251 (1978).

[18] V. Heine and R. O. Jones, J. Phys. C 2, 719 (1969).

[19] J. F. Vetelino, S. P. Gaur, and S. S. Mitra, Phys. Rev. B 5, 2360 (1972).

[20] W. Harrison, Electronic Structure and Properties of Solids (Freeman, San Francisco, 1980).

[21] M. L. Cohen and T. K. Bergstresser, Phys. Rev. 141, 789 (1966).